Endocrine (2012) 41:309–319
DOI 10.1007/s12020-011-9521-y

ORIGINAL ARTICLE

A mathematical model of calcium and phosphorus metabolism in two forms of hyperparathyroidism

J. F. Raposo · A. Pires · H. Yokota · H. G. Ferreira

Received: 30 May 2011 / Accepted: 11 August 2011 / Published online: 27 August 2011

Abstract Parathyroid hormone (PTH) plays a critical role in calcium and phosphorus metabolism. Interestingly, in two forms of hyperparathyroidism (excessive amount of PTH in the serum), the metabolic disturbances in patients with chronic kidney disease (CKD) significantly differ from those with primary hyperparathyroidism (PHP). Since an intuitive understanding of these PTH-linked regulatory mechanisms are hardly possible, we developed a mathematical model using clinical data (1586 CKD and 40 PHP patients). The model was composed of a set of ordinary differential equations, in which the regulatory mechanism of PTH together with other key factors such as 1,25-Dihydroxyvitamin D ($1,25(OH)_2D$) and calcium was described in the tissues including bone, the kidney, the serum, and the parathyroid glands. In this model, an increase in PTH was induced by its autonomous production in PHP, while PTH in CKD was elevated by a decrease in feedback inhibition of $1,25(OH)_2D$ in the serum, as well as an increase in stimulation by phosphorus in the serum. The model-based analysis revealed characteristic differences in the outcomes of hyperparathyroidism in CKD and PHP. The calcium exchange in bone, for instance, was predicted significantly higher in PHP than CKD. Furthermore, we evaluated the observed and predicted responses to the administration of calcimimetics, a recently developed synthetic drug that modulated efficacy of calcium-sensing receptors. The results herein support the notion that the described model would enable us to pose testable hypotheses about the actions of PTH, providing a quantitative analytical tool for evaluating treatment strategies of PHP and CKD.

Keywords Hyperparathyroidism · Mathematical model · Calcium and phosphorus metabolism · Epidemiology

J. F. Raposo
APDP-Portuguese Diabetes Association, Lisbon, Portugal

J. F. Raposo
Department of Public Health, Medical School, New University of Lisbon, Lisbon, Portugal

A. Pires
Department of Nephrology, Hospital Fernando Fonseca, Lisbon, Portugal

H. Yokota (✉)
Department of Biomedical Engineering, Indiana University Purdue University Indianapolis, SL220C, 723 West Michigan Street, Indianapolis, IN 46202, USA
e-mail: hyokota@iupui.edu

H. G. Ferreira
REQIMTE, Department of Chemistry, New University of Lisbon, Lisbon, Portugal

Introduction

The physiological system that regulates the balances of calcium and phosphorus in our body comprises a large number of regulatory components as well as a complex network of molecular and cellular interactions [1]. Since simple, logical reasoning is seldom possible, building mathematical models and conducting computational simulations are often useful to our understanding of a mechanism of actions of key regulatory factors. We have previously developed two versions of mathematical models for calcium and phosphorus metabolism, focusing on the role of parathyroid hormone (PTH) and $1,25(OH)_2D$ with and without inclusion of the role of FGF23 [1, 2]. These models were able to explain the transient alterations in the concentrations of calcium in the serum and the urine by considering a rapid exchangeable pool of calcium (~ 100 mmol). However, the

previous models did not take into account a potential variation in the secretory mass of the parathyroid glands or the balance of calcium and phosphorus in bone. An inclusion of bone remodeling in the model increases the exchangeable amount of calcium approximately by 300-fold. Thus, the existing models were not suited for interpreting some of the clinical data that presented abnormality in the secretion of PTH or bone metabolism.

The study herein aimed to develop a refined mathematical model that would be capable of simulating the alterations in the parathyroid glands and bone remodeling. In particular, we focused on two forms of hyperparathyroidism in which the amount of PTH in the serum was anomalously elevated. One of such disorders was chronic kidney disease (CKD), while the other was primary hyperparathyroidism (PHP). These two forms of hyperparathyroidism result from unrelated causes for the elevation of PTH, and the symptoms of these patients differ. The described model was validated as to whether it would be able to correctly predict each of the characteristic responses in calcium and phosphorus metabolism in the serum and the urine. Since the total amounts of calcium and phosphorus are considered in this extended model, it is possible to evaluate both transient and chronic responses.

In formulating mathematical expressions, we employed observable state variables such as glomerular filtration rates (GFRs), the serum concentrations of PTH, $1,25(OH)_2D$, calcium, and phosphorus, and the urinary excretions of calcium and phosphorus. Besides the calcium and phosphorus balances in the serum and the urine, we also included two sub-compartments corresponding to the parathyroid glands and bone (bone forming osteoblasts and bone degrading osteoclasts). The rates of growth and degradation as well as the functional status of these compartments were subject to the regulatory factors (e.g., PTH, $1,25(OH)_2D$, calcium, and phosphorus) [3–7]. In interpreting clinical data, we used the procedure taken by Parfitt and co-workers [8–13]. We did not include the data for FGF23, bone mineral density, or bone mineral content because of their limited availability.

The specific aim of the current study was to build a mathematical model for calcium and phosphate metabolism, focusing on the regulatory roles of PTH and $1,25(OH)_2D$. The predictive model was then applied to the two forms of hyperparathyroidism (CKD and PHP) and the concentrations of calcium and phosphate in the serum and the urine were evaluated. Furthermore, we examined potential effects of the administration of calcimimetics to patients with hyperparathyroidism. Calcimimetics is a recently developed class of drugs, which is considered to modulate the action of calcium-sensing receptors [14, 15]. These calcium-sensing receptors are located not only in the parathyroid gland but also in the intestine and the kidney tubule [16]. We hypothesized that potential therapeutic strategies differ to patients with CKD and PHP because of the regulatory mechanisms for the induction of hyperparathyroidism. Through the examination of the predicted outcomes in response to calcimimetics, we investigated a possible contribution of the calcium-sensing receptors located in the parathyroid glands, the intestine, and the kidney tubule.

Materials and methods

Clinical data from the patients with CKD

The use of the archived and the collected data obeyed a study protocol, which was approved by the review boards of each of the institutions. Using the laboratory procedures described previously [2], the following data were obtained from a pool of 1586 CKD patients with stable renal function: GFR measured by the creatinine clearance; the serum concentrations of PTH, $1,25(OH)_2D$, calcium, and phosphorus; and the urinary output of calcium and phosphorus. Note that GFR was obtained from the calculation of the 24 h creatinine clearance, since its estimates with a statistical formula cannot be used to compute fractional excretions. The obtained values of the creatinine clearances were normalized to 1.73 m^2 of the body surface area using the Mosteller formula [17]. Calcium and phosphorus excretions were measured in 24 h urine samples (mg/24 h). They were expressed as the ratios of calcium and phosphorus clearances, respectively, to creatinine clearance, which were independent of urinary volume. Each patient was represented by a single set of values collected on the same morning, and the urine collections were started on the previous morning. Regarding medications, 4% of the patients were having calcium supplements and patients on vitamin D or cinacalcet were excluded from the analysis.

Clinical data from the patients with PHP

Retrospective data of 40 consecutive patients (33 females and 7 males) with a mean age at diagnosis of 55.6 ± 2.9 years, who had surgery for PHP were collected. Most patients had an asymptomatic form of this disease and were followed in the same hospital for a mean period of 390 ± 95 days before surgery and up to 6 months after surgery. During this period, clinical and laboratory data were obtained from the patients' records. No patient was submitted to treatment with calcimimetics (including cinacalcet). The patients with GFRs lower than 60 ml/min were excluded to rule out a possibility of secondary hyperparathyroidism. For each patient, we obtained the serum concentrations of PTH, $1,25(OH)_2D$, calcium, and phosphorus. Whenever possible, we also collected data for

the 24 h urinary excretions of calcium and phosphorus together with GFR (evaluated with the Cockcroft–Gault formula). Since the values for ionized (free) calcium were available for a limited number of the patients, we used the amount of total calcium in the mathematical model. Note that the amount of ionized calcium is assumed to be approximately half of the total calcium.

Data processing

To characterize the relationships among clinical data, we examined any correlations between a pair of measured variables such as GFR and $1,25(OH)_2D$. For each pair, one variable was chosen as an independent (driving) variable, which was sorted in the ascending order and smoothed out with a sliding average using 3–5 consecutive values (CKD data) and 10 consecutive values (PHP data) [18]. Furthermore, outliers were removed using the procedure described previously [19]. Using SPSS 16.0 software, the processed data were partitioned into frequency bins, and the means and their standard errors were calculated. Consequently, the raw clinical data were converted into a list of mean values and standard errors of the mean in each of the frequency bins. Note that in CKD and PHP data processing, GFR and the concentrations of PTH in the serum were used as the chief driving variables, respectively.

Systems diagram with compartments

With reference to the systems diagram with varying compartments (Fig. 1), we included 4 additional compartments to 11 original compartments in the previous model. The original compartments were: 4 compartments in the serum (calcium pool—[$Q_{s(Ca)}$], phosphate pool—[$Q_{s(P)}$], PTH—[$Q_{s(PTH)}$], and $1,25(OH)_2D$—[$Q_{s(D)}$]); 2 compartments in bone (calcium pool—[$Q_{b(Ca)}$], and phosphorus pool—[$Q_{b(P)}$]); and 5 compartments in other tissues (intracellular phosphate pool—[$Q_{c(P)}$], 1α-hydroxylase in the kidney—[$Q_{k(E)}$], $1,25(OH)_2D$-dependent intestinal calcium transporter—[$Q_{i(TCa)}$], external balance-dependent phosphate kidney transporter—[$Q_{k(TP)}$], and secretory mass of the parathyroid gland ($Q_{PT(C)}$)] [1, 2].

In the present study, 4 additional compartments were considered. They were 2 compartments in the parathyroid glands ([$Q_{PT(sec)}$], and [$Q_{PT(qui)}$]); and 2 compartments in bone (bone-forming osteoblast cells [Q_{ob}], and bone-degrading osteoclast cells [Q_{oc}]). First, two compartments in the parathyroid glands enabled us to describe long-term perturbations of calcium and phosphate homeostasis closely linked to hyperparathyroidism. Second, the inclusion of 2 bone-related compartments allowed us to evaluating calcium and phosphorus homeostasis through bone remodeling in a relatively long time scale (in the order of 1 month to years) as well as a more rapid exchange of calcium and phosphorus (in the order of 1 h).

Mathematical formulation

The rates of change of the above pools were equated to the algebraic sum of the corresponding inward and outward fluxes. Mathematical expressions are shown in Appendix. We considered three kinetic models such as a linear-diffusional model, a Michaelis–Menten model, and a hyperbolic tangent model. Here are some examples. First, the linear-diffusional model was used to approximate a passive calcium transport process in the intestine. Second, the Michaelis–Menten model was employed to simulate a feedback inhibition process of the synthesis of $1,25(OH)_2D$. Third, the hyperbolic tangent function was, for instance, applied to model inhibition of a PTH release by calcium in the serum.

Numerical simulation

The model was encoded in the Madonna language (University of California, Berkeley), and the computations were conducted in three modules: the differential equation module describing dynamical behaviors of the compartments; the auxiliary equation module defining the fluxes into and out of the compartments, and the reference state module providing the initial steady-state values of the dynamical variables using the parameter values listed in Table 1. These parameter values were derived based on existing data as well as heuristic parameter fitting [1]. A perturbation to a specific state variable was introduced around a steady-state reference, and the dynamical system responses were evaluated. The source codes will be made available upon request.

To simulate the action of calcimimetics, we referred to the study published previously [20]. The affinity of calcium to the calcium-sensing receptor as well as the amount of PTH secretion were estimated using clinical PTH data, and the predicted effects of calcimimetics on each of the three locations of the calcium-sensing receptors (i.e., parathyroid glands, intestine, and kidney tubule) were evaluated. Note that in this simulation a potential effect of calcimimetics on the proliferation of parathyroid gland cells was not included.

Results

Analysis of clinical data from the patients with CKD and PHP

The data from the patients with CKD exhibited a clear correlation of the selected variables to GFR (Fig. 2).

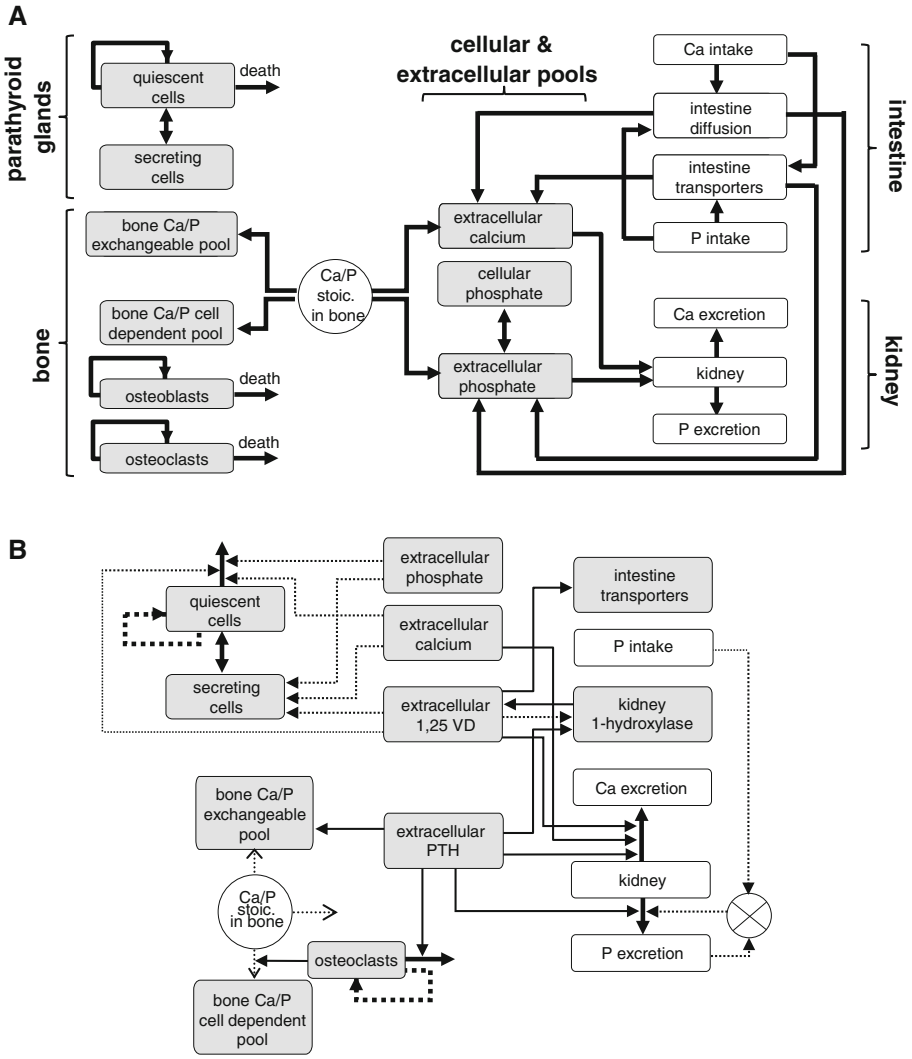

Fig. 1 Schematic illustration of the compartmental model of calcium and phosphorus metabolism. **a** Flux diagram including the parathyroid glands, bone, cellular and extracellular pools, the intestine, and the kidney. Two modules (the parathyroid glands and bone) were added in the described model. The *shaded boxes* represent the pools. **b** Positive (*solid lines*) and negative (*dotted lines*) feedback loops

Among six variables, two variables (concentrations of $1,25(OH)_2D$ and calcium in the serum) showed a positive correlation to GFR. Four other variables (concentrations of PTH and phosphorus in the serum, and the excreted fraction of calcium and phosphorus in the urine) presented a negative correlation to GFR. Small deviations from the observed trends were detected in the calcium concentration in the serum at a normal GFR (Fig. 2c) as well as the urinary excretion of phosphorus at a low GFR (Fig. 2f).

The similar data analysis was conducted for the patients with PHP using the level of PTH in the serum as an independent variable (Fig. 3). Data showed a clear tendency in which an increase in PTH elevated the calcium level in the serum, while it reduced the phosphorus level in the serum. Both the secretions of calcium and phosphorus in the urine were increased together with an elevation of PTH. Although these two sets of data in CKD and PHP patients presented an excess amount of PTH, the mechanism for PTH elevation was apparently different.

Evaluation of calcium balances in the patients with CKD and PHP

Using the mathematical model with the data from the patients with CKD and PHP, we next evaluated calcium balance as a function of PTH concentration in the serum (Fig. 4). The external and internal balances are depicted in Fig. 4a and b, respectively, based on the calcium exchanges through the urinary output and bone remodeling. The results demonstrated that at the same concentration of PTH in the serum, the calcium exchanges through the kidney and bone were significantly higher in the patients with PHP than those with CKD. The comparison between CKD and PHP also indicated that an increase in the PTH level in the serum reduced the fractional content of calcium in bone severer in PHP than CKD (Fig. 4c).

As a potential cause for these differences, we examined a potential role of affinity of a PTH receptor in the calcium

Table 1 Values of the parameters and the reference states

Symbol	Remark	Value
$Q_{ob}0$	Total number of Ob	3.36×10^8 (–)
$Q_{oc}0$	Total number of Oc	$0.1 \times Q_{ob}0$ (–)
$J_{oc}0$	Rate of Oc production	2.0×10^5 (1/h)
$J_{ob}0$	Rate of Ob production	2.0×10^6 (1/h)
$K_{b(Ca)}$	Fraction of Ca turnover in bone	0.1 (1/year)
$J_{ob(Ca)}R$	Ca flux (dependent on Ob)	2.5 (mM)
$J_{oc(Ca)}R$	Ca flux (dependent on Oc)	35 (pg/ml)
$J_{oc(Ca)}S$	Ca flux sensitivity (dependent on Oc)	0.05 $(pg/ml)^{-1}$
$Q_{b(Ca)}0$	Ca pool in bone	3.25×10^4 (mmol)
Fr_{act}	Fraction of secreting PT cells	0.2 (–)
k_{act}	Rate of PT cell activation	0.03 (1/h)
$k_{mult}0$	Rate of PT cell multiplication ([Ca, P, VD]-dependent)	0.03 (–)
$K_{mult(Ca)}R$	Ca affinity (inhibiting PT cell growth)	2.4 (mM)
$k_{mult(Ca)}S$	Ca sensitivity (inhibiting PT cell growth)	1.2 (1/mM)
$k_{mult(D)}R$	VD affinity (inhibiting PT cell growth)	190 (pg/ml)
$k_{mult(D)}S$	VD sensitivity (inhibiting of PT cell growth)	0.03 (1/pg/ml)
$k_{mult(P)}R$	P affinity (stimulating PT cell growth)	1.55 (mM)
Q_{PT} Lim	Max. number PT cells can grow	10 (–)
R_{ob-oc}	Ratio of Ob/Oc pools	10 (–)
$k_{mult(P)}S$	P sensitivity (stimulating PT cell growth)	1 (1/mM)
$Q_{PT}0$	Total number of PT cells	1.0×10^8 (–)
$J_{oc(Ca)\text{-}PTH0}$	Normalized Ca flux (dependent on Oc)	1 (–)

Ob osteoblast, *Oc* osteoclast, *VD* $1,25(OH)_2$ Vitamin D, *PT* parathyroid gland

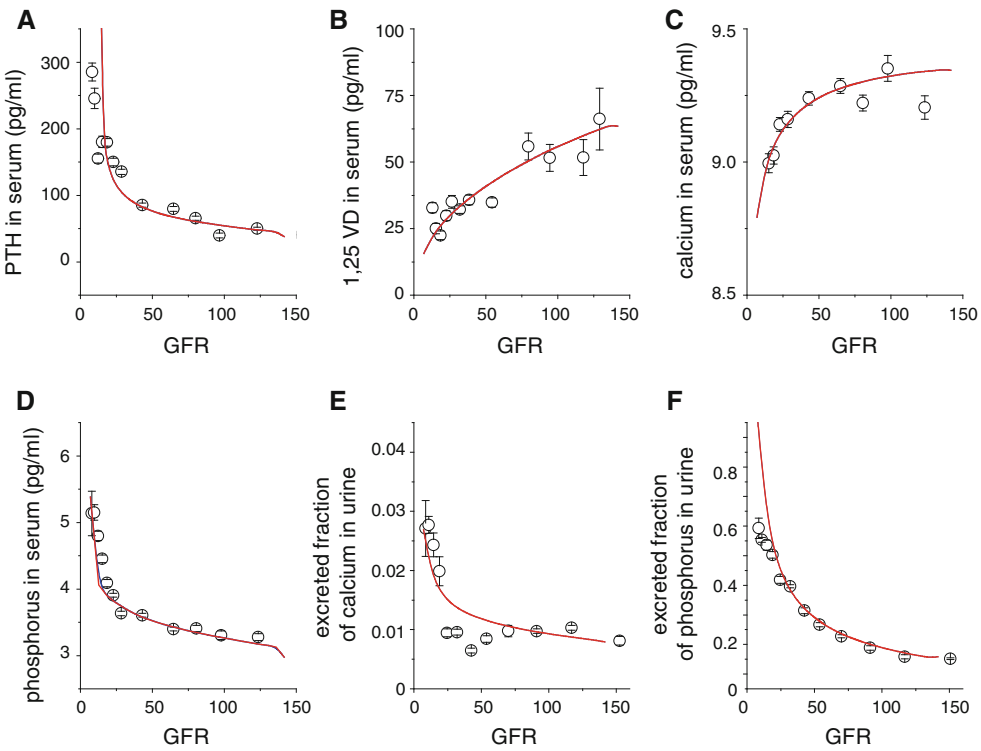

Fig. 2 Analysis of the clinical data of the patients with CKD as a function of GFR. The *open circles* represent the mean value in the frequency bins, while the *solid line* indicates the modeling results. Note that *N* is the number of data points. **a** PTH concentration in the serum ($N = 607$). **b** $1,25(OH)_2D$ concentration in the serum ($N = 206$). **c** Calcium concentration in the serum ($N = 718$). **d** Phosphorus concentration in the serum ($N = 736$). **e** Excreted fraction of calcium in the urine ($N = 305$). **f** Excreted fraction of phosphorus in the urine ($N = 303$)

level in bone (Fig. 4d). A higher affinity significantly decreased the fractional content of calcium in bone, suggesting that the observed differences could result from differential affinities of PTH to bone in CKD and PHP, although other regulatory mechanisms would also be possible.

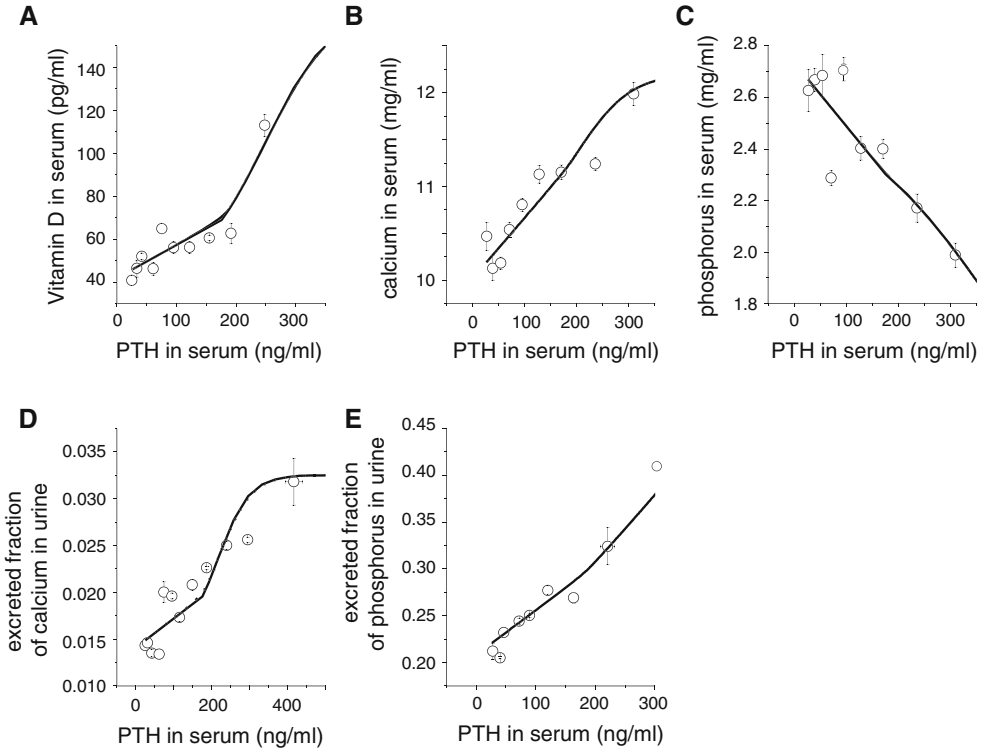

Fig. 3 Analysis of clinical data of the patients with PHP as a function of PTH in the serum. The *open circles* represent the mean value in the frequency bins, while the *solid line* indicates the modeling results. Note that *N* is the number of data points. **a** Vitamin D concentration in the serum ($N = 80$). **b** PTH concentration in the serum ($N = 213$). **c** Phosphorus concentration in the serum ($N = 207$). **d** Excreted fraction of calcium in the urine ($N = 62$). **e** Excreted fraction of phosphorus in the urine ($N = 54$)

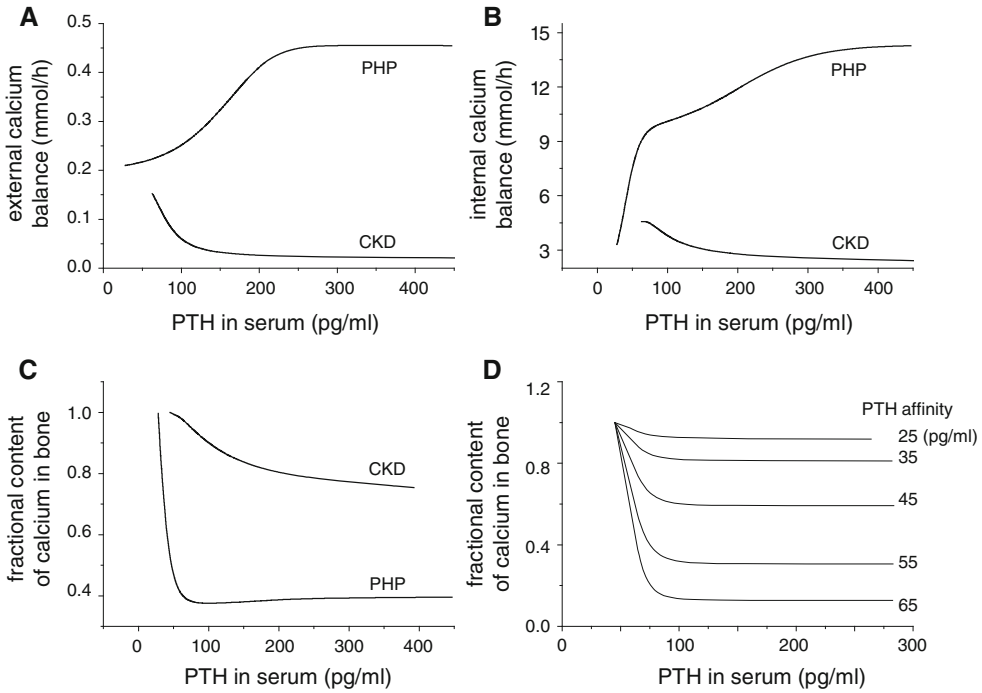

Fig. 4 Simulation results of calcium balance for the patients with CKD and PHP. **a** External calcium balance for CKD and PHP patients. **b** Internal calcium balance for CKD and PHP patients. **c** Fractional content of calcium in bone for CKD and PHP patients. **d** Fractional content of calcium in bone as a function of PTH concentrations in the patients with CKD using affinity of a PTH receptor in bone as a parameter

Predicted outcomes in response to the administration of a calcimimetic

Using the described model, we next examined the effects in response to the administration of calcimimetics (Fig. 5). Note that calcimimetics, i.e., type II calcium receptor agonists, work as allosteric modulators, and they require the presence of calcium to activate the receptor. The observed and simulated data for CKD and PHP are shown (Fig. 5). Note that the condition "PT" represents the predicted outcomes of calcimimetics that was effective only in the parathyroid cells, while the condition "PT–I–K" designates the predicted outcomes effective in the parathyroid cells, the intestine, and the kidney.

In the simulation for the patients with CKD (Fig. 5a), the major effect in "PT" was the alteration in the PTH concentration in the serum with a slight increase in the phosphorus concentration. In "PT–I–K" where calcimimetics was effective to the calcium-sensing receptors in the parathyroid cells, the intestine, and the kidney, we observed a smaller reduction of the PTH concentration and a markedly increase in the urinary excretion of calcium together with a reduction in the calcium concentration in the serum.

Regarding the predictions for the patients with PHP (Fig. 5b), under "PT" in which calcimimetics was effective only in the parathyroid glands, the fractional fall in the PTH concentration in the serum was smaller than the predictions for CKD. When the effects of calcimimetics on the intestine and the kidney were included in "PT–I–K", the alteration of the PTH concentration was smaller than that for CKD with a substantial increase in the urinary excretion of calcium and a small fall in the serum calcium.

Lastly, a long-term simulation for a period of 12 years was conducted for a hypothetical CKD patient, who presented a low GFR (initially 20% of a normal value). Although the residual GFR was maintained at the initial 20% level after a renal failure, the PTH concentration in the serum continually rose chiefly because the functional mass of the parathyroid glands gradually increased. When calcimimetics was administered in 10 years after the renal failure, the model predicted a sudden, substantial fall in the PTH concentration in the serum followed by its gradual elevation.

Discussion

We described the extended mathematical model for analyzing calcium and phosphorus metabolism. Two major extensions from the previous models were the refinement of the states of the parathyroid glands, and the inclusion of a large pool of calcium and phosphorus involved in bone remodeling. The former allowed us to evaluate the role of PTH in metabolic disorders such as PHP, while the latter enabled to predict the chronic responses in CKD (in the order of 1 month to years) including the extended pool of calcium in bone. With these new features in the extended

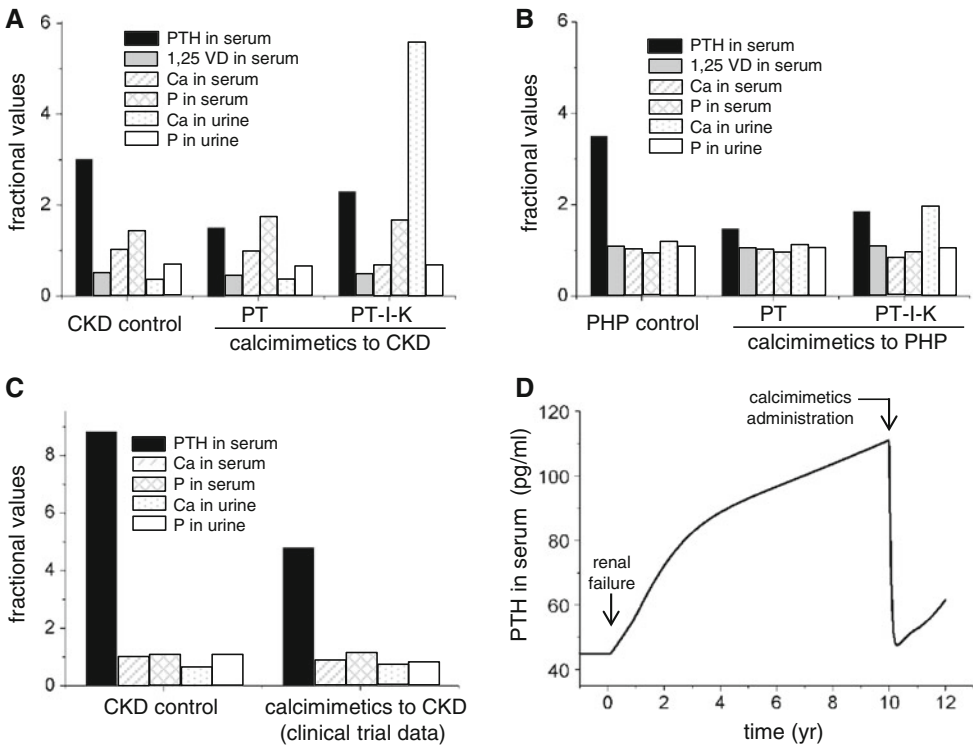

Fig. 5 Predicted outcomes in response to the administration of calcimimetics. The condition "PT" represents the simulation considering the effect of calcimimetics only in the parathyroid gland cells, while the condition "PT–I–K" designates the simulation considering the effects of calcimimetics in the parathyroid gland cells, the intestine, and the kidney. **a** Predicted responses in the patients with CKD. **b** Predicted responses in the patients with PHP. **c** Clinical data in response to the administration of calcimimetics [20]. **d** Simulated temporal evolution of PTH concentrations with the onset of renal failure ($t = 0.2$ years) followed by the administration of calcimimetics ($t = 10$ years)

model, we examined the role of PTH in calcium and phosphorus homeostasis using the clinical data from the patients with CKD and PHP. In both forms of hyperparathyroidism, the level of PTH in the serum was simulated with the distinctively different mechanism of its elevation.

The present study revealed a number of aspects that distinguished the hyperparathyroidism of CKD and of PHP. First, the most striking difference was that the calcium turnover was significantly higher in PHP than CKD. Our prediction is consistent with clinical data showing that a turnover ratio of calcium in bone is 0.006 per year for CKD and 0.13 per year for PHP. Second, several feedback loops regulating the levels of $1,25(OH)_2D$, calcium, and phosphorus in the serum were dynamically affecting the level of PTH in CKD, but the elevated PTH level in the serum in PHP was not primarily resulted from those feedback signals. Instead, those loops oppositely functioned so as to suppress hyperparathyroidism but virtually no effective outcome was observed. Third, in the computational simulation for evaluating the responses to the administration of calcimimetics, the predicted therapeutic outcomes were markedly different in the two forms of hyperparathyroidism (CKD and PHP). Our simulation results indicated that the major effect of calcimimetics might be targeted to the calcium-sensing receptor in the parathyroid glands. These observations, possibly deduced in the past on an intuitive basis, were quantitatively validated through the described model-based analysis. Although basic molecular interactions are included in the described mathematical model, it does not completely represent complex, physiological phenomena in mineral metabolism. The predicted responses to the administration of calcimimetics present a testable hypothesis, which can be examined in pre-clinical studies. Note that the difference in the sample numbers in CKD and PHP is due to the different prevalence of those disorders and availability of patients. Additional clinical data in PHP should be useful to interpret the described model-based predictions.

Because of the complex functional structure, any mathematical model might be regarded as a simplification of the system that regulates the balances of calcium and phosphorus in the human body. For instance, we presented another version of the model that included a feedback loop representing the controlled secretion of FGF23, a phosphaturic hormone [21]. FGF23 was formulated to lower the renal threshold for phosphorus, inhibit the production of $1,25(OH)_2D$ in the kidney as well as the production of PTH. In the current study we did not encode the molecular mechanisms involved in the action of FGF23 or bone mineralization [22], since clinical epidemiological data were not available.

PTH has multiple functions in our body, and bone is a highly dynamic structure in which structural and functional differences exist in cortical and trabecular bones. In this article we identified quantifiable state variables related to hyperparathyroidism, and evaluated the clinically relevant aspects of calcium and phosphorus metabolism treating bone as a single entity. The predictions from the described model as well as further analysis regarding the role of FGF23 in the two forms of hyperparathyroidism and inclusion of more detailed features in bone remodeling [23] should warrant our better understanding of hyperparathyroidism and development of therapeutic strategies for CKD and PHP.

In conclusion, hyperparathyroidism is an excess amount of PTH in the serum that causes various health problems including kidney diseases, osteoporosis, and joint disorders. The described model provides a mathematical framework for predicting and evaluating effects of potential therapeutic agents prior to and during clinical trials. It contributes to a fundamental understanding of physiology of hyperparathyroidism as well as calcium and phosphate metabolism in bone and the kidney. A further evaluation of the role of PTH in concert to FGF23 is needed to translate the current basic knowledge to clinical practice.

Acknowledgments The authors would like to thank the patients and healthy subjects who willingly participated in the study. This project was supported in part by research and development funds from Indiana University Purdue University Indianapolis.

Conflict of interest The authors declare that there is no conflict of interest that could be perceived as prejudicing the impartiality of the research reported.

Appendix

Rate changes of the pools

In the described mathematical model, six differential equations regarding the parathyroid glands and bone remodeling were added to the original model (1):

$$\mathrm{d}(Q_{\mathrm{ob}})/\mathrm{d}t = J_{\mathrm{ob}} - k_{\mathrm{ob}} \cdot Q_{\mathrm{ob}} \quad \text{(proliferation and degradation of osteoblasts)} \tag{1}$$

$$\mathrm{d}(Q_{\mathrm{oc}})/\mathrm{d}t = J_{\mathrm{oc}} - k_{\mathrm{oc}} \cdot Q_{\mathrm{oc}} \quad \text{(proliferation and degradation of osteoclasts)} \tag{2}$$

$$\mathrm{d}\left(Q_{\mathrm{bc(Ca)}}\right)/\mathrm{d}t = J_{\mathrm{ob(Ca)}} - J_{\mathrm{oc(Ca)}} \quad \text{(calcium pool in bone)} \tag{3}$$

$$\mathrm{d}\left(Q_{\mathrm{bc(P)}}\right)/\mathrm{d}t = \beta\left(J_{\mathrm{ob(Ca)}} - J_{\mathrm{oc(Ca)}}\right) \quad \text{(phosphorus pool in bone; } \beta = 5/3 \text{ in hydroxyapatite)} \tag{4}$$

$$\mathrm{d}\left(Q_{\mathrm{PT(act)}}\right)/\mathrm{d}t = k_{\mathrm{act}} \cdot Q_{\mathrm{PT(inact)}} - k_{\mathrm{inact}} \cdot Q_{\mathrm{PT(act)}} \quad \text{(pool of secreting parathyroid gland cells)} \tag{5}$$

$$\mathrm{d}\left(Q_{\mathrm{PT(inact)}}\right)/\mathrm{d}t = k_{\mathrm{inact}} \cdot Q_{\mathrm{PT(act)}} + \left(k_{\mathrm{mult}} - k_{\mathrm{act}} - k_{\mathrm{apo}}\right) \cdot Q_{\mathrm{PT(inact)}} \left(\text{pool of non - secreting parathyroid gland cells}\right) \tag{6}$$

Modeling of bone remodeling and the parathyroid glands

Osteoblasts and osteoclasts were assumed to be produced (J_{ob}, J_{oc}) and degraded (k_{ob}·Q_{ob}, k_{oc}·Q_{oc}) at known rates (k_{ob}, k_{oc}), respectively (4). The osteoblast and osteoclast activities are represented by their ability to store ($J_{\mathrm{ob(Ca)}}$) or mobilize ($J_{\mathrm{oc(Ca)}}$) calcium per cell. We assumed that the osteoclast activity was stimulated by PTH following a hyperbolic tangent model.

The cells of the parathyroid glands were assumed to be in two functional states corresponding to two pools: non-dividing, secreting cells ($Q_{\mathrm{PT(sec)}}$), and potentially dividing or quiescent cells, ($Q_{\mathrm{PT(qui)}}$). A continuous interchange between the two pools as well as a continuous rate of production of quiescent cells was assumed. Furthermore, we included a continuous rate of cell death (k_{apo}) under the inhibition of the serum calcium and 1,25(OH)$_2$D as well as the stimulation of the serum phosphorus (5–10). The conversion rates between active and inactive as well as the multiplication and death rates of the parathyroid cells can be written as fluxes:

$$J_{\mathrm{PT(sec)}} = k_{\mathrm{act}} \cdot Q_{\mathrm{PT(qui)}} - k_{\mathrm{inact}} \cdot Q_{\mathrm{PT(sec)}} \tag{7}$$

$$J_{\mathrm{PT(qui)}} = k_{\mathrm{inact}} \cdot Q_{\mathrm{PT(sec)}} + \left(k_{\mathrm{mult}} - k_{\mathrm{act}} - k_{\mathrm{apo}}\right) \cdot Q_{\mathrm{PT(qui)}} \tag{8}$$

$$J_{\mathrm{PT(mult)}} = k_{\mathrm{mult}} \cdot Q_{\mathrm{PT(qui)}} \cdot Q_{\mathrm{PT}}\_R \tag{9}$$

$$J_{\mathrm{PT(apo)}} = k_{\mathrm{apo}} \cdot Q_{\mathrm{PT(qui)}} \cdot Q_{\mathrm{PT}}\_R \tag{10}$$

The factor Q_{PT}_R, the fraction of the parathyroid cell pool capable of dividing, was introduced since the size of the parathyroid glands tends to a limit (15).

$$Q_{\mathrm{PT}} = Q_{\mathrm{PT(sec)}} + Q_{\mathrm{PT(qui)}} \tag{11}$$

$$Q_{\mathrm{PT}}\_R = (Q_{\mathrm{PT}}M - Q_{\mathrm{PT}})/Q_{\mathrm{PT}}M \tag{12}$$

$$Q_{\mathrm{PT}}M = Q_{\mathrm{PT}}\mathrm{Lim} \cdot Q_{\mathrm{PT}}0 \tag{13}$$

The functional dependence of the multiplication rates of the parathyroid cells on the serum calcium and 1,25(OH)2D ($k_{\mathrm{mult(D)}}$, $k_{\mathrm{mult(Ca)}}$) were assumed to be decreasing sigmoid functions while the dependence on the serum phosphorus ($k_{\mathrm{mult(P)}}$) is assumed to be an increasing sigmoid function.

$$\mathrm{Mult}_{(\mathrm{D})}0 = \left(1 - \tanh\left(k_{\mathrm{mult(D)}}S \cdot \left(C_{\mathrm{s(DH)}}0 - k_{\mathrm{mult(D)}}R\right)\right)\right)^{N\_\mathrm{D}} \tag{14}$$

$$\mathrm{D\_Mult} = 1/\mathrm{Mult}_{(\mathrm{D})}0 \tag{15}$$

$$\mathrm{Mult}_{(\mathrm{D})} = \left(1 - \tanh\left(k_{\mathrm{mult(D)}}S \cdot \left(C_{\mathrm{s(DH)}} - k_{\mathrm{mult(D)}}R\right)\right)\right)^{N\_\mathrm{D}} \tag{16}$$

$$k_{\mathrm{mult(D)}} = \mathrm{D\_Mult} \cdot \mathrm{Mult}_{(\mathrm{D})} \tag{17}$$

$$\mathrm{Mult}_{(\mathrm{Ca})}0 = \left(1 - \tanh\left(k_{\mathrm{mult(Ca)}}S \cdot \left(C_{\mathrm{s(Ca)}}0 - k_{\mathrm{mult(Ca)}}R\right)\right)\right)^{N\_\mathrm{Ca}} \tag{18}$$

$$\mathrm{Ca\_Mult} = 1/\mathrm{Mult}_{(\mathrm{Ca})}0 \tag{19}$$

$$\mathrm{Mult}_{(\mathrm{Ca})} = \left(1 - \tanh\left(k_{\mathrm{mult(Ca)}}S \cdot \left(C_{\mathrm{s(Ca)}} - k_{\mathrm{mult(Ca)}}R\right)\right)\right)^{N\_\mathrm{Ca}} \tag{20}$$

$$k_{\mathrm{mult(Ca)}}0 = \mathrm{Ca\_Mult} \cdot \mathrm{Mult}_{(\mathrm{Ca})}0 \tag{21}$$

$$k_{\mathrm{mult(Ca)}} = \mathrm{Ca\_Mult} \cdot \mathrm{Mult}_{(\mathrm{Ca})} \tag{22}$$

$$\mathrm{Mult}_{(\mathrm{P})}0 = \left(1 + \tanh\left(k_{\mathrm{mult(P)}}S \cdot \left(C_{\mathrm{s(P)}}0 - k_{\mathrm{mult(P)}}R\right)\right)\right)^{N\_\mathrm{P}} \tag{23}$$

$$\mathrm{P\_Mult} = 1/\mathrm{Mult}_{(\mathrm{P})}0 \tag{24}$$

$$\mathrm{Mult}_{(\mathrm{P})} = \left(1 + \tanh\left(k_{\mathrm{mult(P)}}S \cdot \left(C_{\mathrm{s(P)}} - k_{\mathrm{mult(P)}}R\right)\right)\right)^{N\_\mathrm{P}} \tag{25}$$

$$k_{\mathrm{mult(P)}}0 = \mathrm{P\_Mult} \cdot \mathrm{Mult}_{(\mathrm{P})}0 \tag{26}$$

$$\mathrm{k}_{\mathrm{mult(P)}} = \mathrm{P\_Mult} \cdot \mathrm{Mult}_{(\mathrm{P})} \tag{27}$$

The multiplication rate of inactive cells (k_{mult}) was given a reference value of $k_{\mathrm{mult}}0$ multiplied by the function ($k_{\mathrm{mult(DCaP)}}$) equal to 1 in the reference state and which is the sum of three components, respectively, dependent on the serum concentrations of calcium (aCa·$k_{\mathrm{mult(Ca)}}$), 1,25(OH)2D (aD·$k_{\mathrm{mult(D)}}$), and phosphorus (aP·$k_{\mathrm{mult(P)}}$) multiplied by their weighting coefficients, respectively, aCa, aD, and aP (assumed to be 1/3).

$$k_{\mathrm{mult(DCaP)}}0 = a\mathrm{D} \cdot k_{\mathrm{mult(D)}}0 + a\mathrm{Ca} \cdot k_{\mathrm{mult(Ca)}}0 + a\mathrm{P} \cdot k_{\mathrm{mult(P)}}0 \tag{28}$$

$$k_{\mathrm{mult(DCaP)}} = a\mathrm{D} \cdot k_{\mathrm{mult(D)}} + a\mathrm{Ca} \cdot k_{\mathrm{mult(Ca)}} + a\mathrm{P} \cdot k_{\mathrm{mult(P)}} \tag{29}$$

$$k_{\mathrm{mult}} = k_{\mathrm{mult}}0 \cdot k_{\mathrm{mult(DCaP)}} \tag{30}$$

The bone cells, actively involved in the movements of calcium, are constantly produced (J_{ob} and J_{oc}) and removed (J_{oc}_Dec) at rates k_{oc} and k_{ob} defined by the equations:

$$k_{\mathrm{oc}} = J_{\mathrm{oc}}0/Q_{\mathrm{oc}}0 \tag{31}$$

$$k_{\mathrm{ob}} = J_{\mathrm{ob}}/Q_{\mathrm{ob}}0 \tag{32}$$

$$J_{oc}\_Dec = k_{oc} \cdot Q_{oc} \quad (33)$$

As a first approximation the rate of production of osteoblasts is assumed to be constant (J_{ob}).

Osteoblasts and osteoclasts are assumed to be responsible for the bone deposition and removal of calcium, respectively. The osteoblast-dependent calcium deposition ($J_{ob\_(Ca)}$) depends on the size of the pool of osteoblast (Q_{ob}) and on the flux per osteoblast ($J_{ob(Ca)\_Cas}$) which depends on the serum concentration of calcium ($J_{ob\_(Ca)\_Cas}f$) assumed to obey Michaelis–Menten kinetics.

$$J_{ob(Ca)}\_kO0 = K_{b(Ca)} \cdot Q_{b(Ca)}0 \quad (34)$$

$$J_{ob(Ca)\_Cas}f0 = C_{s(Ca)}0/\left(C_{s(Ca)}0 + J_{b(Ca)\_Cas}R\right) \quad (35)$$

$$J_{ob(Ca)\_Cas}M = J_{ob(Ca)}0/J_{ob(Ca)\_Cas}f0 \quad (36)$$

$$k_{ob\_Ca} = J_{ob(Ca)}\_kO0/Q_{ob}0 \quad (37)$$

$$J_{ob\_(Ca)\_Cas}f = C_{s(Ca)}/\left(C_{s(Ca)} + J_{ob\_(Ca)\_Cas}R\right) \quad (38)$$

$$J_{ob(Ca)\_Cas} = J_{ob(Ca)\_Cas}M \cdot J_{ob(Ca)\_Cas}f \quad (39)$$

$$J_{ob\_(Ca)} = k_{ob(Ca)} \cdot J_{ob(Ca)\_Cas} * Q_{ob} \quad (40)$$

The osteoclast-dependent calcium mobilization ($J_{oc(Ca)}$) is a function of the size of the osteoclast pool (Q_{oc}) and is a function of the serum concentration of PTH ($J_{oc(Ca)\text{-}PTHf}$). R_{ob-oc} is the ratio between the osteoclast and the osteoblast pools.

$$J_{oc(Ca)-PTHf0} = 1 + \tanh\left(J_{oc(Ca)-PTH-S} \cdot \left(C_{s(PTH)0} - J_{oc(Ca)-PTH-R}\right)\right) \quad (41)$$

$$J_{oc(Ca)-PTH-M} = J_{oc(Ca)-PTH0}/\left(J_{oc(Ca)-PTHf0} \cdot Q_{b(Ca)}0\right) \quad (42)$$

$$J_{oc(Ca)-PTHf} = 1 + \tanh\left(J_{oc(Ca)-PTH-S} \cdot \left(C_{s(PTH)} - J_{oc(Ca)-PTH-R}\right)\right) \quad (43)$$

$$J_{oc(Ca)-PTH} = J_{oc(Ca)-PTH-M} \cdot J_{oc(Ca)-PTHf} \cdot Q_{b(Ca)} \quad (44)$$

$$K_{oc(Ca)} = R_{ob-oc} \cdot K_{ob(Ca)} \quad (45)$$

$$J_{oc(Ca)} = K_{oc(Ca)} \cdot J_{oc(Ca)-PTH} \cdot Q_{oc} \quad (46)$$

$$Q_{b(P)}0 = \beta \cdot Q_{b(Ca)}0 \quad (47)$$

$$J_{b(Ca)-OS} = -J_{ob(Ca)} + J_{oc(Ca)} \quad (48)$$

$$J_{b(P)-OS} = \beta \cdot J_{b(Ca)-OS} \quad (49)$$

The kidney functional mass, reduced by a pathological process as in CKD, is assumed to be proportional to the glomerular filtration rate.

References

1. J.F. Raposo, L.G. Sobrinho, H.G. Ferreira, A minimal mathematical model of calcium homeostasis. J. Clin. Endocrinol. Metab. **87**, 4330–4340 (2002)
2. A. Pires, T. Adragão, M.J. Pais, J. Vinhas, H.G. Ferreira, Inferring disease mechanisms from epidemiological data in chronic kidney disease: calcium and phosphorus metabolism. Nephron Clin. Pract. **112**, c137–c147 (2009)
3. A.M. Parfitt, M.K. Drezner, F.H. Glorieux, J.A. Kanis, H. Malluche, P.J. Meunier, S.M. Ott, R.R. Recker, Bone histomorphometry: standardization of nomenclature, symbols, and units Report of the ASBMR Histomorphometry Nomenclature Committee. J. Bone Miner. Res. **2**, 595–610 (1987)
4. A.M. Parfitt, Bone-forming cells in clinical conditions, in *Bone. Volume 1: the osteoblast and osteocyte*, ed. by B.K. Hall (Telford Press and CRC Press, Boca Raton, FL, 1990), pp. 351–429
5. A.M. Parfitt, D. Willgoss, J. Jacobi, H.M. Lloyd, Cell kinetics in parathyroid adenomas: evidence for decline in rates of cell birth and tumour growth, assuming clonal origin. Clin. Endocrinol. (Oxf) **35**, 151–157 (1991)
6. A.M. Parfitt, G.D. Braunstein, A. Katz, Radiation-associated hyperparathyroidism: comparison of adenoma growth rates, inferred from weight and duration of latency, with prevalence of mitosis. J. Clin. Endocrinol. Metab. **77**, 1318–1322 (1993)
7. A.M. Parfitt, Parathyroid growth: normal and abnormal, in *The Parathyroids—Basic and Clinical Concepts*, ed. by J.P. Bilezikian (Raven Press, New York, 1994), pp. 373–405
8. Q. Wang, S. Palnitkar, A.M. Parfitt, Parathyroid cell proliferation in the rat: effect of age and of phosphate administration and recovery. Endocrinology **137**, 4558–4562 (1996)
9. A.M. Parfitt, Q. Wang, S. Palnitkar, Rates of cell proliferation in adenomatous, suppressed, and normal parathyroid tissue: implications for pathogenesis. J. Clin. Endocrinol. Metab. **83**, 863–869 (1998)
10. D.S. Rao, M. Honasoge, G.W. Divine, E.R. Philips, M.W. Lee, Mo, M.R. Ansari, G.B. Talpos, A.M. Parfitt, Effect of vitamin D nutrition on parathyroid adenoma weight: pathogenetic and clinical implications. J. Clin. Endocrinol. Metab. **85**, 1054–1058 (2000)
11. A.M. Parfitt, Parathyroid hormone and periosteal bone expansion. J. Bone Miner. Res. **17**, 1741–1743 (2002)
12. S. Qiu, D.S. Rao, S. Palnitkar, A.M. Parfitt, Relationships between osteocyte density and bone formation rate in human cancellous bone. Bone **31**, 709–711 (2002)
13. A.M. Parfitt, Misconceptions (3): calcium leaves bone only by resorption and enters only by formation. Bone **33**, 259–263 (2003)
14. T.B. Drueke, E. Ritz, Treatment of secondary hyperparathyroidism in CKD patients with cinacalcet and/or Vitamin D derivatives. Clin. J. Am. Soc. Nephrol. **4**, 234–241 (2009)
15. P. Evenepoel, Calcimimetics in chronic kidney disease: evidence, opportunities and challenges. Kidney Int. **74**, 265–275 (2008)
16. E.M. Brown, R.J. MacLeod, Extracellular calcium sensing and extracellular calcium signaling. Physiol. Rev. **81**, 240–297 (2001)
17. R.D. Mosteller, Simplified calculation of body-surface area. N. Engl. J. Med. **317**, 1098 (1987)
18. A. Hald, Designs of sampling investigations and experiments, in *Statistical Theory with Engineering Applications*, 1st edn. (Wiley, New York, 1952), pp. 510
19. N. Weiss, Descriptive measures, in *Elementary statistics*, 5th edn., ed. by G. Tobin (Addison Wesley, Boston, 2002), pp. 120–121
20. C. Charytan, J.W. Coburn, M. Chonchol, J. Herman, Y.H. Lien, W. Liu, P.S. Klassen, L.C. McCary, V. Pichette, Cinacalcet hydrochloride is an effective treatment for secondary hyperparathyroidism in patients with CKD not receiving dialysis. Am. J. Kidney Dis. **46**, 58–67 (2005)
21. Y. Yokota, J.F. Raposo, A. Chen, C. Jiang, H.G. Ferreira, Evaluation of the role of FGF23 in mineral metabolism. Gene Regul. Syst. Biol. **3**, 131–142 (2009)

22. V. Lemaire, F.L. Tobin, L.D. Greller, C.R. Cho, L.J. Suva, Modeling the interactions between osteoblast and osteoclast activities in bone remodeling. J. Theor. Biol. **229**, 293–309 (2004)
23. T. Bellido, A.A. Ali, L.I. Plotkin, Q. Fu, I. Gubrij, P.K. Roberson, R.S. Weinstein, C.A. O'Brien, S.C. Manolagas, R.L. Jilka, Proteasomal degradation of Runx2 shortens parathyroid hormone-induced anti-apoptotic signaling in osteoblasts. A putative explanation for why intermittent administration is needed for bone anabolism. J. Biol. Chem. **278**, 50259–50272 (2003)